A&A 423, 919–924 (2004)
DOI: 10.1051/0004-6361:20035770

Astronomy & Astrophysics

Triggered star formation in the inner wing of the SMC. Two possible supernova explosions in the N83-84-85 region⋆

E. Bratsolis[1,2], M. Kontizas[2], and I. Bellas-Velidis[3]

[1] École Nationale Supérieure des Télécommunications, Département Traitement du Signal et des Images, 46 rue Barrault, 75013 Paris, France
e-mail: bratsoli@tsi.enst.fr
[2] Department of Astrophysics, Astronomy and Mechanics, Faculty of Physics, University of Athens, 15783 Athens, Greece
[3] National Observatory of Athens, Institute of Astronomy and Astrophysics, Lofos Koufou - P. Penteli, 15236 Athens, Greece

Received 1 December 2003 / Accepted 3 May 2004

Abstract. In this article we study the N83-84-85 region of the inner wing of the SMC. Direct and low-dispersion objective prism plates taken with the 1.2 m UK Schmidt Telescope have been digitized by the SuperCOSMOS machine. Star counts have been performed for our region in selected luminosity slices in the *U* filter and isodensity contours have been used to identify the structures with enhanced stellar number density. We find evidence of triggered star formation from massive stars of older to more recent OB associations. Circular arcs constructed by O and B stars have been detected. A study of the population places stars with more recent ages in the groups of the arcs than of their centers. These effects can be explained by supernova explosions. A catalogue of the non-saturated detected OB stars in this region is given.

Key words. techniques: image processing – methods: data analysis – stars: formation – galaxies: Magellanic Clouds – shock waves

1. Introduction

The formation of massive stars is a topic of major interest. Massive stars are often formed in groups, such as OB associations and clusters. Massive stars finish their life by supernova explosions. The interstellar medium (ISM) is continuously stirred by supernova explosions and stellar winds of massive stars. Shock waves from supernova and stellar wind-blown bubbles around O and B type star associations generate turbulences in the ISM. Star formation may trigger further star formation in nearby gas if the density is high enough but also star-forming clouds are destroyed by the same effects and shut off star formation. There remains an open question about the density of the ISM and the violence of the effect. A supernova explosion can produce a shell wall or a dense interstellar cloudlet only if the density is high enough.

In this work we use data from digitized plates, using the direct and objective prism, of the SMC focusing on the inner wing. The same region has been studied by Testor & Lortet (1988). Our study with automated techniques of the objective prism plates (Bratsolis et al. 1998, 2000; Bratsolis 2002) gave OB populations in circular structures. A new study to investigate plates of the same region with slices of different populations and contour detection (Maragoudaki et al. 2001) showed that the outer populations of OB stars are more recent OBs of the centers. This is evidence of star-formation triggered by supernova explosions. Therefore, there is a strong correlation of our study region with the supernova remnants (SNRs) of *ROSAT* X-ray observations No. 223 RX J0112.7-7207 and No. 245 RX J0119.4–7301 (Kahabka et al. 1999). These regions were searched for in IRAS and ISO (for lambda 170). The image of the SMC in both cases is of low resolution.

Following the theoretical work of Vishniac (1994), Elmegreen (1994) and Ehlerová et al. (1997) for isolated supernova explosions we can extract a time scale for the supernova explosions and the density of the ISM before the explosion.

2. The region N83-84-85 of the SMC

The region N83-84-85 belongs to the inner wing of the SMC and is of interest because of its OB associations and nebulae. It is evident that there is a correlation between associations like NGC 456, 460a, b and 465 with the nebulae of ionized gas. This region has been studied by different authors in the past (Westerlund 1961; Azzopardi & Vigneau 1982; Kontizas et al. 1988; Testor & Lortet 1987; Lortet & Testor 1988; Dapergolas et al. 1991; Caplan et al. 1996). There are groups of stars with age variations of 4−10 Myr and spatial scales of 30−400 pc. There is also an extended region containing N83-84-85 with a diameter of more than 500 pc and sequential star formation on a scale of 10^7 yr which seems to be part of a supergiant shell

⋆ Table 3 is only available in electronic form at http://www.edpsciences.org

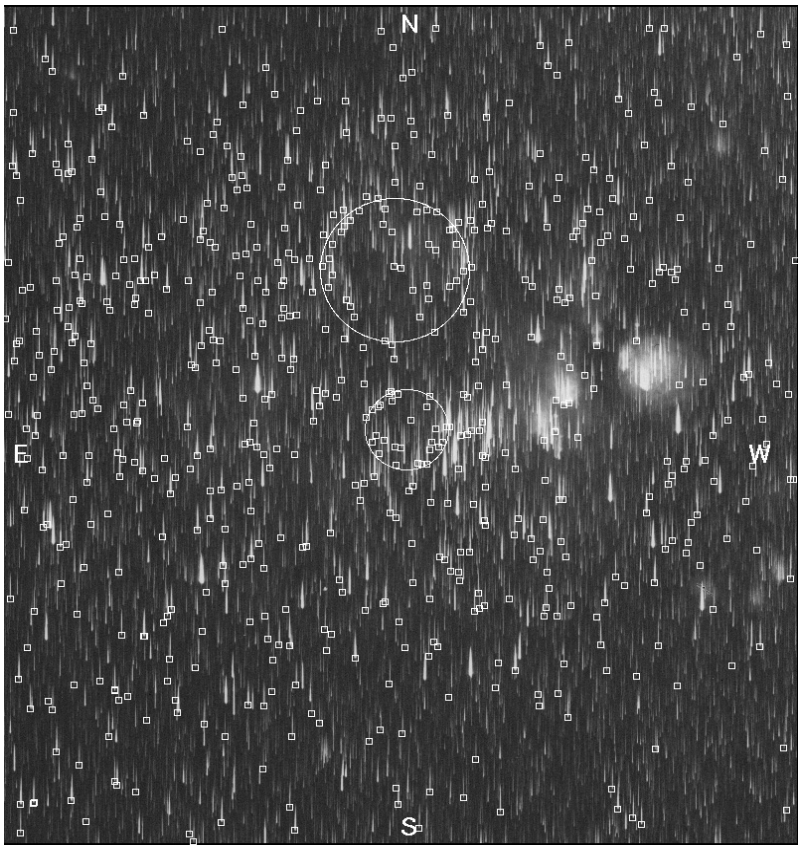

Fig. 1. Positions of OB classified stars with an automated method of correlation. The circles present the regions of SN explosions.

(Westerlund 1961; Staveley-Smith et al. 1997; Stanimirović et al. 1999).

We focus on this region because it seems to show a feedback between OB star formation and the physical properties of the ISM. It suggests that star formation and ISM properties probably are self-regulated. The ISM is continuously stirred by supernova explosions and stellar winds. The shock waves engaged by the supernova accelerate galactic cosmic rays that penetrate deeply into molecular clouds and clumps and heat and ionize them. Far ultraviolet photons are produced by massive star formation and photoinize the less dense surface regions of the molecular cloud and its internal clumps.

3. Image reduction

Our test image contains a region of 36.2 × 39.1 arcmin^2 of SMC. The scanning pixel size of the SuperCOSMOS measuring machine is 10 μm and the plate scale is 67.11 arcsec/mm. Our image is centered at $RA_{2000} = 1^h16^m$ and $Dec_{2000} = -73°20'$ and contains a region from $RA_{2000} = 1^h12^m$ to $RA_{2000} = 1^h20^m$ and from $Dec_{2000} = -73°35'$ to $Dec_{2000} = -73°05'$. The magnitude limit for classification of our plate is $m_B = 18.5$.

The detection (DETSP), extraction (EXTSP) and classification (RCORR) was made by automated methods (Bratsolis et al. 1998, 2000; Bratsolis 2002).

The extracted spectra are stored in a two-dimensional file $n \times 128$, where n is the number of detected spectra. Each row of this file is an independent normalized spectrum with a length of 128 pixels. The maximum correlation method has been used to automatically classify the spectra and gave 610 clearly classified OB spectra (Fig. 1).

The same region was also chosen from the direct U plate taken with the UK 1.2 m Schmidt Telescope. The plate was digitized by the SuperCOSMOS machine and the derived data given for the detected images positions and magnitudes. Isodensity contours have been used to identify the various structures with enhanced stellar density. The contour level separation has been defined by the mean value plus 3σ from the local background (Fig. 2). The detected stellar images were divided in various luminosity slices according to their magnitude. The magnitude limit for the U plate is $m_U = 19.7$, corresponding to the A0 spectral type stars.

The data were separated in four luminosity slices.

The first slice contains main sequence stars with $U < 15$ and $-1.5 < U - V < -0.8$, corresponding to ages less than 8×10^6 yr and stars more luminous than B2 spectral type.

The second slice contains main sequence stars with $15 < U < 16$ and $-1.4 < U - V < -0.6$, corresponding to ages of 8×10^6–1.2×10^7 yr and stars of B2 spectral type.

The third slice contains main sequence stars with $16 < U < 17$ and $-1.3 < U - V < -0.2$, corresponding to ages of 1.2–3×10^7 yr and stars of late B2 to early B4 spectral type.

The fourth slice contains main sequence stars with $U > 17$ and $-1.1 < U - V$ corresponding to ages grater than 3×10^7 yr.

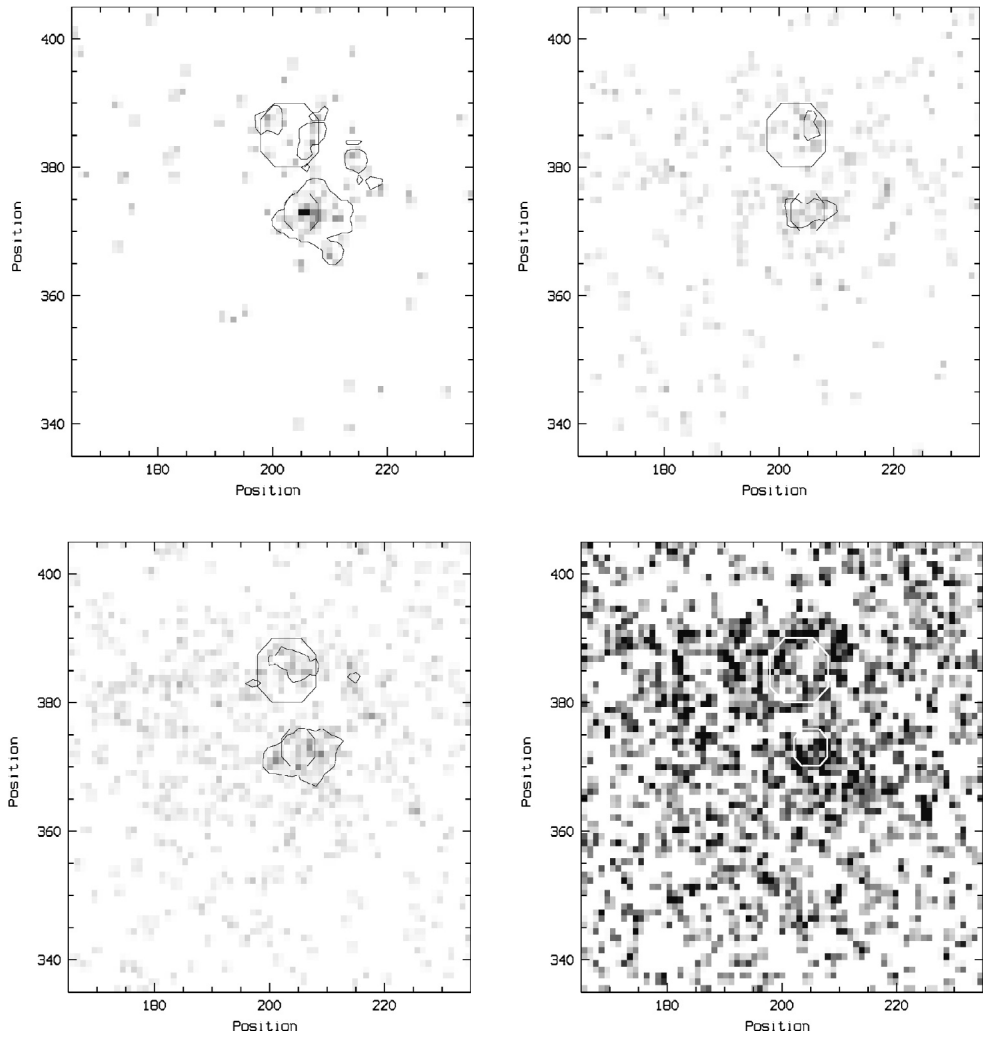

Fig. 2. *Upper left*: isodensity contours for main sequence OB stars younger than 8×10^6 yr. *Upper right*: isodensity contours for main sequence B stars with ages between 8×10^6 and 1.2×10^7 yr. *Lower left*: isodensity contours for main sequence B stars with ages between 1.2×10^7 and 3×10^7 yr. *Lower right*: density distribution for main sequence B stars with ages older than 3×10^7 yr. The octagons present the regions of SN explosions. Subslices for these star ages do not give any significant contours.

The scale calibration of the U plate, produced for the SMC distance modulus $m - M = 19$ and based on theoretical models, is given in Table 1.

Detected objects in our region (not including the OB stars) are presented by Bica & Schmitt (1995) in Table 2. The non-saturated detected OB stars are presented in Table 3.

Table 1. Scale calibration of the U plate for the SMC.

Spectral type	$U_{\rm SMC}$	Age
O5	11.9	3×10^6
B0	13.5	4×10^6
B1	14.6	6×10^6
B2	15.4	1×10^7
B3	16.3	1.5×10^7
B4	16.7	2.8×10^7
B5	17.2	4×10^7
B6	17.5	1×10^8
B7	17.9	1.6×10^8
B8	18.4	2×10^8
B9	18.5	3×10^8
A0	19.7	4×10^8

4. The evolution of an expanding shell

Let us accept a simple model of a supernova explosion. The supernova produces a gravitational instability in the ISM and accumulates the gas in an expanding shell. The expanding shell's equations are known as Sedov's equations (Dyson & Williams 1997), given by

$$R(t) = \left(\frac{25}{3\pi}\right)^{1/5} \left(\frac{E_{\rm SN}}{\rho_0}\right)^{1/5} t^{2/5} \quad (1)$$

and

$$u_{\rm s}(t) = \frac{2}{5}\frac{R(t)}{t} \quad (2)$$

where $R(t)$ is the radius of the shell and $u_{\rm s}(t)$ the expansion velocity of the shell at the time t relative to the ambient medium with density ρ_0. $E_{\rm SN}$ is the total supernova explosion energy.

Table 2. Detected objects in our region according Bica & Schmitt (1995).

Number	RA(2000) h m s	Dec(2000) ° ′ ″	Name	*x*Pos.	*y*Pos.	Type	*D*max (′)	*D*min (′)	Remarks
887	01 12 52	−73 07 10	*L*91	223	391	*C*	1.20	1.20	
894	01 13 48	−73 17 33	*NGC*456	218	376	*NA*	3.80	2.90	
895	01 13 50	−73 18 02	*S MC* − *N*83*A*	218	376	*NC*	0.60	0.45	in *NGC*456
896	01 13 52	−73 15 45	*S MC* − *N*83*B*	217	379	*NC*	0.30	0.30	att *NGC*456
898	01 13 53	−73 15 56	*L*61 − 501	217	379	*NC*	0.25	0.25	att *NGC*456
899	01 13 53	−73 24 59	*HW*68	218	366	*C*	0.55	0.55	
901	01 13 56	−73 15 53	*MA*1779	217	379	*NC*	0.25	0.25	att *NGC*456
902	01 14 00	−73 15 12	*L*61 − 502	217	380	*NC*	0.30	0.30	
903	01 14 02	−73 17 05	*S MC* − *N*83*C*	216	377	*NC*	0.90	0.90	in *NGC*456
906	01 14 06	−73 14 06	*B*146	216	381	*A*	0.75	0.75	att *S MC* − *N*84*n*
907	01 14 17	−73 22 42	*HW*69	215	369	*C*	0.55	0.55	
908	01 14 18	−73 15 50	*S MC* − *N*84*C*	215	379	*NC*	0.65	0.65	att *S MC* − *N*84*n*
909	01 14 22	−73 14 04	*S MC* − *N*84*n*	214	381	*NA*	4.00	3.00	
910	01 14 24	−73 14 03	*L*61 − 505	214	381	*NC*	0.35	0.30	in *N*84*n*
914	01 14 37	−73 16 24	*BS* 161	213	378	*NA*	1.60	1.20	in *S MC* − *N*84*s*
916	01 14 38	−73 17 59	*NGC*460*nw*	213	376	*NA*	1.90	1.70	in *S MC* − *N*84*s*
917	01 14 38	−73 18 27	*S MC* − *N*84*A*	213	375	*NC*	0.80	0.65	in *NGC*460*nw*
918	01 14 41	−73 18 30	*L*61 − 507	213	375	*NC*	0.30	0.30	in *NGC*460*nw*
923	01 14 45	−73 18 18	*MA*1794	212	375	*NA*	0.70	0.70	in *NGC*460*nw*
924	01 14 45	−73 20 44	*S MC* − *N*84*D*	212	372	*NC*	0.30	0.30	in *NGC*460*se*
925	01 14 45	−73 22 54	*BS* 165	212	369	*AC*	0.95	0.65	
926	01 14 46	−73 18 54	*S MC* − *N*84*s*	212	374	*NA*	7.50	4.00	
927	01 14 47	−73 19 45	*S MC* − *N*84*B*	212	373	*NC*	0.35	0.35	in *NGC*460*se*
928	01 14 47	−73 21 04	*BS* 166	212	371	*NC*	0.45	0.35	in *NGC*460*se*
929	01 14 47	−73 20 12	*MA*1796	212	372	*NC*	0.20	0.20	in? *NGC*460*se*, *PN*?
931	01 14 52	−73 07 04	*B*147	211	391	*AC*	1.20	1.10	
932	01 14 54	−73 20 02	*MA*1799	211	373	*NA*	0.60	0.55	in *NGC*460*se*
933	01 14 54	−73 19 45	*NGC*460*se*	211	373	*NA*	2.60	1.50	in *S MC* − *N*84*s*
934	01 14 57	−73 19 36	*L*61 − 512	211	373	*NA*	0.50	0.35	in *NGC*460*se*
946	01 15 32	−73 11 46	*S MC* − *DEM*155	207	384	*NA*	1.80	1.80	in *S MC* − *DEM*157
947	01 15 42	−73 10 00	*HW*72	206	386	*CN*	0.55	0.45	in *S MC* − *DEM*157
948	01 15 42	−73 19 46	*NGC*465	207	373	*A*	5.00	4.00	in *S MC* − *DEM*157
949	01 15 49	−73 20 40	*Sk*157	206	372	*C*	0.60	0.60	in *NGC*465
950	01 15 52	−73 18 56	*Sk*158	206	374	*C*	0.70	0.60	in *NGC*465
952	01 16 09	−73 11 19	*S MC* − *DEM*156	203	385	*NA*	2.80	2.60	in *S MC* − *DEM*157
954	01 16 21	−73 20 12	*S MC* − *DEM*157	203	372	*NA*	22.00	17.00	
956	01 16 48	−73 09 36	*HW*74	199	387	*C*	0.55	0.50	in *S MC* − *DEM*158
957	01 16 49	−73 09 20	*S MC* − *DEM*158	199	387	*NA*	1.80	1.50	in *S MC* − *DEM*157
958	01 16 59	−73 12 06	*S MC* − *DEM*159	198	383	*NA*	1.50	0.80	in *S MC* − *DEM*157
959	01 17 30	−73 34 09	*HW*75	197	352	*CA*	0.90	0.80	
961	01 19 31	−73 05 38	*B*156	183	392	*C*	0.65	0.45	

After the linear analysis of Elmegreen (1994) and Vishniac (1994) in a uniform medium with gravitation constant G, we have that an expanding shell with surface density Σ and velocity dispersion in the shell c has an instantaneous maximum growth rate ω given by

$$\omega = -\frac{3u_s}{R} + \sqrt{\frac{u_s^2}{R^2} + \left(\frac{\pi G\Sigma}{c}\right)}. \quad (3)$$

If ρ and ρ_0 are the densities of the perturbed and unperturbed medium respectively, then they are connected to the dimensionless quantity $\mathcal{M}$ by the formula (Efremov & Elmegreen 1998)

$$\frac{\rho}{\rho_0} = \left(\frac{u_s}{c}\right)^2 = \mathcal{M}^2. \quad (4)$$

At the time t_b, when $\omega > 0$ or

$$\xi = \frac{\sqrt{8}u_s c}{\pi G R \Sigma} < 1 \quad (5)$$

the perturbation grows.

We now use the same logic as Ehlerová et al. (1997) for isolated supernova explosions and we obtain the radius

$$R(t) = 83.2\left(\frac{E_{SN}}{10^{51}\ \mathrm{erg}}\right)^{1/5}\left[\left(\frac{\mu}{1.3}\right)^{-1}\left(\frac{n_0}{\mathrm{cm}^{-3}}\right)^{-1}\right]^{1/5} \left(\frac{t}{\mathrm{Myr}}\right)^{2/5}\ \mathrm{pc} \quad (6)$$

the total mass

$$m(R) = \frac{4\pi\rho_0 R^3(t)}{3} \quad (7)$$

and the surface density

$$\Sigma(t) = \frac{m(R)}{4\pi R^2(t)}. \quad (8)$$

From Eqs. (8), (7) and (6) we have

$$\Sigma(t) = 0.91\left(\frac{E_{\rm SN}}{10^{51}\ {\rm erg}}\right)^{1/5}\left[\left(\frac{\mu}{1.3}\right)^4\left(\frac{n_0}{{\rm cm}^{-3}}\right)^4\right]^{1/5} \left(\frac{t}{\rm Myr}\right)^{2/5} M_\odot/{\rm pc}^2. \quad (9)$$

From Eqs. (5), (2) and (9) we have

$$\xi(t) = 0.89\frac{c}{G}\frac{1}{\left(\rho_0^4 E_{\rm SN}\right)^{1/5}} t^{-7/5}. \quad (10)$$

The instability time $t_{\rm b}$ is estimated by the condition

$$\xi(t_{\rm b}) = 1 \quad (11)$$

and is

$$t_{\rm b} = 21.9\left(\frac{c}{1\ {\rm km\,s^{-1}}}\right)^{5/7}\left(\frac{n_0}{{\rm cm}^{-3}}\right)^{-4/7}\left(\frac{\mu}{1.3}\right)^{-4/7} \left(\frac{E_{\rm SN}}{10^{51}\ {\rm erg}}\right)^{-1/7} {\rm Myr}. \quad (12)$$

The radius R and the expansion velocity $u_{\rm s}$ of the shell at $t_{\rm b}$ are

$$R(t_{\rm b}) = 286\left(\frac{c}{1\ {\rm km\,s^{-1}}}\right)^{2/7}\left(\frac{n_0}{{\rm cm}^{-3}}\right)^{-3/7}\left(\frac{\mu}{1.3}\right)^{-3/7} \left(\frac{E_{\rm SN}}{10^{51}\ {\rm erg}}\right)^{1/7} {\rm pc} \quad (13)$$

and

$$u_{\rm s}(t_{\rm b}) = \frac{2}{5}\frac{R(t_{\rm b})}{t_{\rm b}} = 5.22\left(\frac{c}{1\ {\rm km\,s^{-1}}}\right)^{-3/7}\left(\frac{n_0}{{\rm cm}^{-3}}\right)^{1/7}\left(\frac{\mu}{1.3}\right)^{1/7} \left(\frac{E_{\rm SN}}{10^{51}\ {\rm erg}}\right)^{2/7} {\rm km\,s^{-1}}. \quad (14)$$

The estimation of fragmentation time is given by

$$\int_{t_{\rm b}}^{t_{\rm f}} \omega(t){\rm d}t = 1. \quad (15)$$

From Eqs. (3) and (5) we obtain

$$\omega = \frac{u_{\rm s}}{R}\left(-3 + \sqrt{1 + \frac{8}{\xi^2(t)}}\right) \quad (16)$$

and from Eqs. (11) and (10)

$$\xi(t) = \left(\frac{t}{t_{\rm b}}\right)^{-7/5}. \quad (17)$$

From Eqs. (15), (17), (16) and (2) we have

$$\int_{t_{\rm b}}^{t_{\rm f}} \frac{-3 + \sqrt{1 + 8\left(\frac{t}{t_{\rm b}}\right)^{14/5}}}{t}{\rm d}t = 1 \quad (18)$$

and

$$\int_1^{x_{\rm f}} \frac{-3 + \sqrt{1 + 8x^{14/5}}}{x}{\rm d}x = \frac{5}{2} \quad (19)$$

where

$$x_{\rm f} = t_{\rm f}/t_{\rm b}. \quad (20)$$

The numerical solution of (19) gives $x_{\rm f} \approx 2.47$. From Eqs. (12) and (20) we have

$$t_{\rm f} = 54.1\left(\frac{c}{1\ {\rm km\,s^{-1}}}\right)^{5/7}\left(\frac{n_0}{{\rm cm}^{-3}}\right)^{-4/7}\left(\frac{\mu}{1.3}\right)^{-4/7} \left(\frac{E_{\rm SN}}{10^{51}\ {\rm erg}}\right)^{-1/7} {\rm Myr}. \quad (21)$$

From Eqs. (21), (6) and (2) we obtain

$$R(t_{\rm f}) = 410.6\left(\frac{c}{1\ {\rm km\,s^{-1}}}\right)^{2/7}\left(\frac{n_0}{{\rm cm}^{-3}}\right)^{-3/7}\left(\frac{\mu}{1.3}\right)^{-3/7} \left(\frac{E_{\rm SN}}{10^{51}\ {\rm erg}}\right)^{1/7} {\rm pc} \quad (22)$$

and

$$u_{\rm s}(t_{\rm f}) = \frac{2}{5}\frac{R(t_{\rm f})}{t_{\rm f}} = 3.04\left(\frac{c}{1\ {\rm km\,s^{-1}}}\right)^{-3/7}\left(\frac{n_0}{{\rm cm}^{-3}}\right)^{1/7} \left(\frac{\mu}{1.3}\right)^{1/7}\left(\frac{E_{\rm SN}}{10^{51}\ {\rm erg}}\right)^{2/7} {\rm km\,s^{-1}}. \quad (23)$$

5. Two possible supernova explosions

As we observe (Fig. 1), the OB stars are not uniformly distributed. They present different densities and holes. Here we chose two cases presenting circular arcs and to explain these as star groups formed by a triggered effect, by the supernova explosions. These approximately circular forms suggest that pre-stellar gas was uniformly swept up by a central source of pressure. We chose two circles with different size.

The small circle has a center at $\mathrm{RA}_{2000} = 1^{\rm h}16^{\rm m}$ and $\mathrm{Dec}_{2000} = -73°20'$ and radius 32.4 pc. On the right part of this circle we find the end of the nebula N84 and on the left part the beginning of the N85.

The large circle has a center at $\mathrm{RA}_{2000} = 1^{\rm h}16^{\rm m}$ and $\mathrm{Dec}_{2000} = -73°11'$ and radius 58.9 pc. At its center we find the association DEM156 and at its circumference the association DEM155, the nebula N86 and the associations DEM158 and DEM159.

Both circles have a radius less than 100 pc, so we can consider isolated supernova explosions. We suppose now that the radii of circles now are not so different from the radius at the fragmentation time. The small circle has a radius $R_1(t_{\rm f})$ and the large circle a radius $R_2(t_{\rm f})$. We also suppose that the average molecule in a cloud is $\mu = 1.3$, the total energy of a supernova is $E_{\rm SN} = 10^{51}$ erg and the velocity dispersion in the shell is $c = 1\ {\rm km\,s^{-1}}$. From Eq. (22) we have

$$R(t_{\rm f}) = 410.6\left(\frac{n_0}{{\rm cm}^{-3}}\right)^{-3/7}\ {\rm pc} \quad (24)$$

which gives

$$n_0 = \left(\frac{R(t_f)}{410.6\ \mathrm{pc}}\right)^{-7/3}\ \mathrm{cm}^{-3}. \quad (25)$$

Equation (25) gives for the small circle a numerical density before the explosion of $n_{01} = 374\ \mathrm{cm}^{-3}$ and for the large circle $n_{02} = 93\ \mathrm{cm}^{-3}$. From our star counts and the derived densities corresponding to the isopleths we have found that in the small circle the number density corresponding to the brightest stars with age about 5×10^6 yr is 14 times the background value whereas in the large circle it is 3.2 times. The ratio of the two is about 5 with 30% error. The ratio in the above theoretical densities is 4. This is a very good result considering the errors. The triggering star formation for the two possible supernova explosions has been verified by using the image of stellar densities. Isodensity contour plots present older B populations at the centers of our study regions (Fig. 2). These populations remain until the slice corresponding to main sequence B stars with ages between 1.2×10^7 and 3×10^7 yr. That means that the two possible supernova explosions occurred about 3×10^7 yr ago.

The diagrams of Fig. 2 are actually isopleths showing all main sequence stars at four levels of magnitude. We indicate at what magnitude level (marked in terms of age, Table 1) the OB stars disappear, as expected. In this case we determine the number of stars per unit pixel by using the values of background b and standard deviation σ. The values used to determine these isopleths are: $b = 0.2$ and $\sigma = 0.29$ stars per pixel for the upper left, $b = 0.59$ and $\sigma = 0.33$ stars per pixel for the upper right, $b = 0.71$ and $\sigma = 0.66$ stars per pixel for the lower left and $b = 1.1$ and $\sigma = 0.68$ stars per pixel for the lower right. The isopleth density is given by $b + 3\sigma$. In the lower right case of Fig. 2 there are no isopleth density contours because the contrast is not high enough.

6. Conclusions

In this paper we attempt to show by a systematic observational method that it is possible to generate the birth of massive OB stars by triggered effects like supernova explosions. We have chosen the region N83-84-85 of the inner wing of SMC and we detected all the non-saturated OB stars in an objective prism plate of this region. We extracted and classified the stars automatically, using a method developed previously by us. The spatial distribution of the OB stars was found to be non-uniform with holes and high density parts that could be explained as star formation regions caused by supernovae. Two possible cases have been studied. The theoretical approach was the same as Ehlerová et al. (1997) but for isolated explosions. From the observations we estimated the radius where the new population is born assuming that the supernova explosions occurred at their centers and from the theoretical equations we extracted the numerical densities of the ISM before the explosions. A study of isopleths of the stellar population of this region, from direct plates at various magnitude slices, provides an estimation of the time when the possible explosions took place. Finally the actual catalogue of the detected OB stars is given.

Acknowledgements. The authors are grateful to ROE for the loan of the observational material. The authors also thank F. Maragoudaki and E. Livanou for the contour programs. M.K. would like to thank the ELKE of the EKPAN (University of Athens) for financial support.

References

Azzopardi, M., & Vigneau, J. 1982, A&AS, 50, 291
Bica, E. L. D., & Schmitt, H. R. 1995, ApJS, 101, 41
Bratsolis, E., Bellas-Velidis, I., Kontizas, E., et al. 1998, A&AS, 133, 293
Bratsolis, E., Bellas-Velidis, I., Dapergolas, A., Kontizas, E., & Kontizas, M. 2000, A&AS, 142, 339
Bratsolis, E. 2002, in Automated Data Analysis in Astronomy, Narosa, ed. R. Gupta, H. P. Singh, & C. A. L. Bailer-Jones, 99
Caplan, J., Taisheng, Ye, Deharveng, L., Turtle, A. J., & Kennicutt, R. C. 1996, A&A, 307, 403
Dapergolas, A., Kontizas, E., Kontizas, M., et al. 1991, A&AS, 87, 97
Dyson, J. E., & Williams, D. A. 1997, The Physics of Interstellar Medium, Second Edition (Bristol, Philadelphia: Institute of Physics Publishing)
Efremov, Y. N., & Elmegreen, B. G. 1988, MNRAS, 299, 643
Elmegreen, B. G. 1994, ApJ, 427, 384
Ehlerová, S., Palous, J., Theis, Ch., & Hensler, G. 1997, A&A, 328, 121
Kahabka, P., Pietsch, W., Filipović, & Heberl, F. 1999, A&AS, 136, 81
Kontizas, E., Morgan, D. H., Kontizas, M., & Dapergolas, A. 1988, A&A, 201, 208
Lortet, M.-C., & Testor, G. 1988, A&A, 194, 11
Testor, G., & Lortet, M.-C. 1987, A&A, 178, 25
Maragoudaki, F., Kontizas, M., Kontizas, E., Dapergolas, A., & Morgan, D. H. 1998, A&A, 338, L29
Stanimirović, S., Staveley-Smith, L., Dickey, J. M., Sault, R. J., & Snowden, S. L. 1999, MNRAS, 302, 417
Staveley-Smith, L., Sault, R. J., Hatzidimitriou, D., Kesteven, M. J., & McConnel, D. 1997, MNRAS, 289, 225
Vishniac, E. T. 1994, ApJ, 428, 186
Westerlund, B. E. 1961, Uppsala Astron. Obs. Ann., 5, 2
Westerlund, B. E. 1997, The Megellanic Clouds, ed. A. King, D. Lin, S. Maran, J. Pringle, & M. Ward (Cambridge University Press)

Online Material

Table 3. Detected (non-saturated) OB stars in our region.

Number	RA(2000) h m s	Dec(2000) ° ′ ″	Number	RA(2000) h m s	Dec(2000) ° ′ ″	Number	RA(2000) h m s	Dec(2000) ° ′ ″
1	01 18 58	–73 37 28	42	01 17 35	–73 32 00	83	01 17 45	–73 28 47
2	01 18 60	–73 37 08	43	01 18 60	–73 31 26	84	01 13 53	–73 30 04
3	01 20 47	–73 36 19	44	01 20 19	–73 30 44	85	01 17 52	–73 28 42
4	01 17 53	–73 37 24	45	01 20 33	–73 30 35	86	01 14 29	–73 29 51
5	01 16 34	–73 37 46	46	01 18 05	–73 31 29	87	01 16 14	–73 29 08
6	01 14 12	–73 38 23	47	01 15 11	–73 32 29	88	01 17 59	–73 28 23
7	01 18 39	–73 36 42	48	01 18 15	–73 31 22	89	01 19 16	–73 27 44
8	01 20 04	–73 36 04	49	01 20 21	–73 30 18	90	01 19 17	–73 27 43
9	01 14 17	–73 38 03	50	01 19 01	–73 30 51	91	01 19 31	–73 27 34
10	01 15 41	–73 37 18	51	01 19 36	–73 30 35	92	01 17 19	–73 28 24
11	01 12 38	–73 38 09	52	01 16 08	–73 31 48	93	01 18 40	–73 27 46
12	01 14 26	–73 37 35	53	01 19 30	–73 30 28	94	01 17 23	–73 28 08
13	01 17 55	–73 36 19	54	01 15 11	–73 31 58	95	01 19 04	–73 27 10
14	01 16 46	–73 36 36	55	01 14 58	–73 31 59	96	01 16 36	–73 28 05
15	01 20 45	–73 34 59	56	01 17 60	–73 30 50	97	01 18 09	–73 27 30
16	01 20 37	–73 34 59	57	01 19 38	–73 30 08	98	01 14 30	–73 28 32
17	01 20 36	–73 34 58	58	01 19 38	–73 30 04	99	01 14 55	–73 28 23
18	01 20 12	–73 35 03	59	01 15 38	–73 31 31	100	01 19 01	–73 26 53
19	01 16 04	–73 36 32	60	01 13 42	–73 32 01	101	01 15 03	–73 28 19
20	01 16 25	–73 36 09	61	01 17 44	–73 30 37	102	01 17 59	–73 27 17
21	01 19 31	–73 34 55	62	01 20 03	–73 29 40	103	01 19 58	–73 26 24
22	01 14 29	–73 36 38	63	01 16 45	–73 30 56	104	01 20 24	–73 26 05
23	01 16 46	–73 35 50	64	01 19 05	–73 29 54	105	01 15 47	–73 27 51
24	01 19 43	–73 34 31	65	01 19 47	–73 29 37	106	01 16 56	–73 27 26
25	01 19 44	–73 34 20	66	01 20 38	–73 29 08	107	01 18 58	–73 26 36
26	01 18 09	–73 34 25	67	01 14 08	–73 31 25	108	01 13 16	–73 28 33
27	01 20 05	–73 33 26	68	01 14 27	–73 31 06	109	01 17 46	–73 27 03
28	01 15 54	–73 34 47	69	01 15 25	–73 30 47	110	01 15 44	–73 27 46
29	01 20 19	–73 32 43	70	01 18 46	–73 29 23	111	01 15 02	–73 27 57
30	01 13 59	–73 34 55	71	01 13 07	–73 31 14	112	01 14 46	–73 27 56
31	01 12 38	–73 35 16	72	01 14 54	–73 30 36	113	01 15 40	–73 27 37
32	01 17 01	–73 33 32	73	01 15 35	–73 30 20	114	01 16 44	–73 27 10
33	01 19 45	–73 32 15	74	01 17 57	–73 29 22	115	01 14 24	–73 27 54
34	01 17 49	–73 32 60	75	01 19 02	–73 28 53	116	01 16 43	–73 27 06
35	01 18 32	–73 32 43	76	01 17 05	–73 29 37	117	01 16 15	–73 27 08
36	01 16 39	–73 33 19	77	01 16 19	–73 29 48	118	01 15 25	–73 27 24
37	01 16 53	–73 33 04	78	01 17 22	–73 29 08	119	01 20 38	–73 25 23
38	01 18 44	–73 32 04	79	01 20 31	–73 27 45	120	01 15 44	–73 27 01
39	01 17 31	–73 32 29	80	01 16 33	–73 29 19	121	01 17 10	–73 26 29
40	01 19 20	–73 31 39	81	01 16 12	–73 29 23	122	01 18 35	–73 25 56
41	01 14 53	–73 33 08	82	01 12 48	–73 30 25	123	01 14 59	–73 27 03

Table 3. continued.

Number	RA(2000) h m s	Dec(2000) ° ′ ″	Number	RA(2000) h m s	Dec(2000) ° ′ ″	Number	RA(2000) h m s	Dec(2000) ° ′ ″
124	01 14 11	–73 27 09	165	01 18 59	–73 23 10	206	01 19 43	–73 20 19
125	01 18 23	–73 25 36	166	01 15 18	–73 24 24	207	01 13 10	–73 22 32
126	01 20 05	–73 24 53	167	01 17 13	–73 23 40	208	01 14 56	–73 21 60
127	01 16 25	–73 26 19	168	01 18 37	–73 23 01	209	01 12 20	–73 22 42
128	01 13 52	–73 27 06	169	01 18 19	–73 23 05	210	01 12 22	–73 22 41
129	01 15 55	–73 26 24	170	01 20 13	–73 22 12	211	01 19 00	–73 20 26
130	01 17 11	–73 25 54	171	01 15 36	–73 23 53	212	01 18 48	–73 20 28
131	01 12 26	–73 27 19	172	01 20 10	–73 22 06	213	01 16 43	–73 21 12
132	01 14 17	–73 26 42	173	01 19 43	–73 22 16	214	01 19 22	–73 20 11
133	01 15 55	–73 25 59	174	01 13 26	–73 24 24	215	01 13 36	–73 22 10
134	01 14 60	–73 26 16	175	01 15 36	–73 23 39	216	01 19 07	–73 20 01
135	01 19 28	–73 24 37	176	01 14 59	–73 23 49	217	01 20 10	–73 19 32
136	01 16 00	–73 25 53	177	01 15 15	–73 23 41	218	01 13 28	–73 21 53
137	01 17 58	–73 25 02	178	01 18 28	–73 22 31	219	01 15 15	–73 21 21
138	01 19 50	–73 24 16	179	01 16 32	–73 23 11	220	01 15 50	–73 21 08
139	01 18 23	–73 24 46	180	01 13 22	–73 24 04	221	01 18 38	–73 20 06
140	01 13 23	–73 26 26	181	01 19 32	–73 21 51	222	01 17 48	–73 20 23
141	01 18 10	–73 24 48	182	01 13 54	–73 23 50	223	01 12 45	–73 21 56
142	01 15 07	–73 25 39	183	01 16 35	–73 22 58	224	01 16 29	–73 20 44
143	01 16 03	–73 25 20	184	01 18 02	–73 22 19	225	01 16 13	–73 20 49
144	01 18 05	–73 24 33	185	01 20 24	–73 21 20	226	01 16 09	–73 20 48
145	01 14 47	–73 25 39	186	01 15 42	–73 22 52	227	01 16 15	–73 20 43
146	01 16 06	–73 25 12	187	01 15 59	–73 22 44	228	01 19 12	–73 19 34
147	01 13 31	–73 25 51	188	01 16 09	–73 22 38	229	01 13 39	–73 21 28
148	01 15 47	–73 25 05	189	01 12 51	–73 23 35	230	01 13 26	–73 21 31
149	01 15 53	–73 25 03	190	01 16 53	–73 22 16	231	01 13 15	–73 21 33
150	01 15 03	–73 25 15	191	01 14 46	–73 22 57	232	01 19 19	–73 19 25
151	01 12 46	–73 25 53	192	01 14 48	–73 22 56	233	01 18 53	–73 19 32
152	01 13 44	–73 25 36	193	01 19 53	–73 21 03	234	01 20 19	–73 18 57
153	01 20 04	–73 23 12	194	01 13 52	–73 23 04	235	01 15 32	–73 20 41
154	01 17 32	–73 24 13	195	01 18 52	–73 21 12	236	01 19 56	–73 18 58
155	01 17 30	–73 24 11	196	01 18 27	–73 21 15	237	01 19 40	–73 19 04
156	01 19 60	–73 23 07	197	01 16 22	–73 21 59	238	01 15 34	–73 20 35
157	01 17 59	–73 23 52	198	01 18 20	–73 21 15	239	01 18 33	–73 19 30
158	01 16 23	–73 24 27	199	01 15 34	–73 22 04	240	01 17 32	–73 19 53
159	01 13 29	–73 25 19	200	01 16 20	–73 21 47	241	01 17 51	–73 19 44
160	01 14 49	–73 24 55	201	01 18 09	–73 21 06	242	01 16 39	–73 20 10
161	01 13 39	–73 25 13	202	01 16 55	–73 21 31	243	01 15 20	–73 20 34
162	01 13 05	–73 25 17	203	01 13 39	–73 22 33	244	01 12 36	–73 21 21
163	01 15 08	–73 24 39	204	01 16 50	–73 21 29	245	01 19 22	–73 19 03
164	01 17 45	–73 23 41	205	01 18 02	–73 20 59	246	01 16 07	–73 20 10

Table 3. continued.

Number	RA(2000) h m s	Dec(2000) ° ′ ″	Number	RA(2000) h m s	Dec(2000) ° ′ ″	Number	RA(2000) h m s	Dec(2000) ° ′ ″
247	01 18 24	–73 19 17	288	01 19 47	–73 17 06	329	01 14 26	–73 17 10
248	01 17 42	–73 19 32	289	01 20 27	–73 16 47	330	01 12 43	–73 17 38
249	01 16 25	–73 19 57	290	01 19 42	–73 17 06	331	01 19 58	–73 14 55
250	01 16 01	–73 20 04	291	01 16 41	–73 18 03	332	01 18 03	–73 15 41
251	01 16 29	–73 19 54	292	01 19 32	–73 16 57	333	01 17 29	–73 15 53
252	01 17 55	–73 19 22	293	01 16 37	–73 17 57	334	01 14 35	–73 16 46
253	01 12 35	–73 20 57	294	01 16 06	–73 18 07	335	01 18 28	–73 15 24
254	01 18 02	–73 19 10	295	01 17 13	–73 17 40	336	01 18 31	–73 15 15
255	01 17 59	–73 19 08	296	01 14 41	–73 18 30	337	01 18 15	–73 15 16
256	01 16 05	–73 19 48	297	01 19 15	–73 16 51	338	01 19 37	–73 14 43
257	01 15 58	–73 19 50	298	01 16 36	–73 17 51	339	01 12 31	–73 17 07
258	01 16 43	–73 19 34	299	01 14 38	–73 18 26	340	01 15 34	–73 16 11
259	01 14 55	–73 20 06	300	01 19 03	–73 16 50	341	01 20 21	–73 14 19
260	01 16 35	–73 19 32	301	01 16 28	–73 17 45	342	01 16 24	–73 15 47
261	01 14 33	–73 20 03	302	01 19 34	–73 16 31	343	01 17 27	–73 15 24
262	01 20 12	–73 17 54	303	01 14 45	–73 18 15	344	01 17 34	–73 15 19
263	01 13 08	–73 20 23	304	01 17 47	–73 17 11	345	01 17 51	–73 15 08
264	01 13 09	–73 20 23	305	01 18 01	–73 17 01	346	01 14 40	–73 16 12
265	01 15 47	–73 19 34	306	01 17 02	–73 17 21	347	01 20 05	–73 14 11
266	01 16 40	–73 19 16	307	01 15 41	–73 17 49	348	01 19 55	–73 14 04
267	01 15 42	–73 19 34	308	01 16 04	–73 17 40	349	01 15 29	–73 15 37
268	01 14 47	–73 19 45	309	01 16 24	–73 17 28	350	01 16 43	–73 15 07
269	01 15 35	–73 19 26	310	01 17 43	–73 16 59	351	01 14 17	–73 15 49
270	01 15 40	–73 19 25	311	01 12 19	–73 18 40	352	01 18 23	–73 14 24
271	01 20 17	–73 17 34	312	01 15 43	–73 17 40	353	01 16 25	–73 15 06
272	01 19 23	–73 17 56	313	01 16 30	–73 17 22	354	01 20 18	–73 13 33
273	01 16 02	–73 19 10	314	01 17 09	–73 17 08	355	01 19 32	–73 13 52
274	01 15 53	–73 19 10	315	01 16 28	–73 17 16	356	01 19 43	–73 13 45
275	01 15 55	–73 19 08	316	01 17 15	–73 16 59	357	01 16 29	–73 14 55
276	01 18 37	–73 18 09	317	01 19 10	–73 16 14	358	01 20 16	–73 13 26
277	01 17 55	–73 18 15	318	01 14 21	–73 17 51	359	01 13 52	–73 15 44
278	01 19 09	–73 17 45	319	01 19 37	–73 15 50	360	01 18 12	–73 14 16
279	01 15 33	–73 19 03	320	01 15 33	–73 17 19	361	01 18 16	–73 14 12
280	01 19 15	–73 17 41	321	01 15 16	–73 17 23	362	01 15 20	–73 15 11
281	01 17 18	–73 18 24	322	01 13 28	–73 17 55	363	01 16 54	–73 14 39
282	01 19 08	–73 17 41	323	01 16 44	–73 16 49	364	01 14 58	–73 15 12
283	01 12 58	–73 19 44	324	01 12 26	–73 18 08	365	01 19 41	–73 13 26
284	01 16 17	–73 18 41	325	01 13 12	–73 17 51	366	01 15 32	–73 14 57
285	01 12 36	–73 19 47	326	01 16 58	–73 16 34	367	01 15 26	–73 14 50
286	01 16 45	–73 18 25	327	01 12 46	–73 17 46	368	01 15 57	–73 14 39
287	01 20 10	–73 16 59	328	01 20 10	–73 15 11	369	01 20 05	–73 13 03

Table 3. continued.

Number	RA(2000) h m s	Dec(2000) ° ′ ″	Number	RA(2000) h m s	Dec(2000) ° ′ ″	Number	RA(2000) h m s	Dec(2000) ° ′ ″
370	01 18 18	–73 13 44	411	01 14 38	–73 13 04	452	01 17 20	–73 10 45
371	01 17 06	–73 14 09	412	01 18 42	–73 11 39	453	01 18 59	–73 10 06
372	01 12 52	–73 15 20	413	01 20 06	–73 10 59	454	01 16 59	–73 10 51
373	01 19 45	–73 12 58	414	01 17 01	–73 12 10	455	01 17 11	–73 10 47
374	01 13 08	–73 15 15	415	01 14 54	–73 12 51	456	01 19 33	–73 09 50
375	01 17 44	–73 13 39	416	01 15 46	–73 12 35	457	01 17 57	–73 10 23
376	01 17 52	–73 13 28	417	01 16 00	–73 12 28	458	01 17 50	–73 10 19
377	01 20 23	–73 12 20	418	01 17 30	–73 11 56	459	01 17 24	–73 10 27
378	01 17 32	–73 13 26	419	01 19 04	–73 11 16	460	01 15 53	–73 10 49
379	01 16 47	–73 13 40	420	01 13 40	–73 13 04	461	01 17 43	–73 10 03
380	01 16 06	–73 13 54	421	01 18 57	–73 11 09	462	01 18 09	–73 09 53
381	01 17 27	–73 13 22	422	01 15 41	–73 12 20	463	01 18 50	–73 09 35
382	01 17 22	–73 13 21	423	01 18 28	–73 11 20	464	01 12 36	–73 11 32
383	01 18 54	–73 12 42	424	01 19 49	–73 10 47	465	01 16 56	–73 10 12
384	01 13 21	–73 14 33	425	01 17 29	–73 11 42	466	01 15 40	–73 10 37
385	01 15 39	–73 13 50	426	01 17 44	–73 11 35	467	01 15 57	–73 10 31
386	01 19 18	–73 12 23	427	01 18 54	–73 11 08	468	01 19 45	–73 09 02
387	01 19 51	–73 12 09	428	01 14 58	–73 12 32	469	01 14 10	–73 11 01
388	01 17 30	–73 13 01	429	01 13 25	–73 12 59	470	01 18 12	–73 09 37
389	01 17 56	–73 12 51	430	01 19 30	–73 10 43	471	01 18 18	–73 09 28
390	01 19 43	–73 12 04	431	01 17 55	–73 11 18	472	01 13 55	–73 10 53
391	01 16 49	–73 13 09	432	01 19 12	–73 10 47	473	01 14 27	–73 10 39
392	01 19 03	–73 12 14	433	01 16 58	–73 11 37	474	01 19 42	–73 08 46
393	01 12 53	–73 14 18	434	01 19 37	–73 10 35	475	01 18 42	–73 09 09
394	01 19 35	–73 11 56	435	01 18 48	–73 10 54	476	01 14 05	–73 10 42
395	01 14 35	–73 13 44	436	01 13 35	–73 12 34	477	01 17 02	–73 09 42
396	01 18 22	–73 12 23	437	01 13 27	–73 12 35	478	01 16 50	–73 09 39
397	01 15 34	–73 13 22	438	01 15 37	–73 11 55	479	01 16 19	–73 09 49
398	01 19 20	–73 11 59	439	01 13 23	–73 12 28	480	01 14 24	–73 10 23
399	01 19 36	–73 11 50	440	01 13 52	–73 12 20	481	01 15 08	–73 10 10
400	01 16 51	–73 12 51	441	01 12 57	–73 12 34	482	01 18 16	–73 09 04
401	01 14 40	–73 13 33	442	01 16 15	–73 11 34	483	01 15 28	–73 10 01
402	01 15 59	–73 13 05	443	01 15 31	–73 11 45	484	01 15 43	–73 09 55
403	01 14 31	–73 13 31	444	01 13 32	–73 12 20	485	01 15 41	–73 09 53
404	01 19 01	–73 11 56	445	01 16 19	–73 11 25	486	01 15 19	–73 09 58
405	01 14 16	–73 13 29	446	01 17 04	–73 11 10	487	01 17 25	–73 09 15
406	01 17 11	–73 12 22	447	01 17 31	–73 10 51	488	01 19 34	–73 08 22
407	01 17 40	–73 12 11	448	01 20 18	–73 09 43	489	01 14 42	–73 10 07
408	01 18 14	–73 11 57	449	01 12 09	–73 12 24	490	01 16 48	–73 09 24
409	01 20 11	–73 11 04	450	01 14 16	–73 11 49	491	01 19 07	–73 08 26
410	01 16 09	–73 12 36	451	01 19 07	–73 10 06	492	01 17 46	–73 08 56

Table 3. continued.

Number	RA(2000) h m s	Dec(2000) ° ′ ″	Number	RA(2000) h m s	Dec(2000) ° ′ ″	Number	RA(2000) h m s	Dec(2000) ° ′ ″
493	01 16 24	–73 09 25	534	01 14 01	–73 08 02	575	01 13 46	–73 05 01
494	01 14 20	–73 10 03	535	01 14 32	–73 07 50	576	01 20 05	–73 02 45
495	01 15 17	–73 09 44	536	01 17 55	–73 06 41	577	01 19 13	–73 03 03
496	01 15 37	–73 09 37	537	01 17 48	–73 06 38	578	01 17 09	–73 03 48
497	01 16 44	–73 09 08	538	01 20 08	–73 05 41	579	01 19 11	–73 02 55
498	01 15 30	–73 09 33	539	01 19 36	–73 05 49	580	01 19 10	–73 02 54
499	01 18 27	–73 08 28	540	01 19 42	–73 05 46	581	01 13 07	–73 04 55
500	01 19 31	–73 07 58	541	01 19 33	–73 05 45	582	01 17 44	–73 03 20
501	01 13 19	–73 10 05	542	01 15 15	–73 07 19	583	01 13 27	–73 04 38
502	01 13 48	–73 09 54	543	01 14 10	–73 07 33	584	01 14 59	–73 04 10
503	01 19 15	–73 07 59	544	01 13 22	–73 07 37	585	01 16 58	–73 03 26
504	01 16 54	–73 08 49	545	01 20 09	–73 05 13	586	01 16 41	–73 03 31
505	01 16 02	–73 08 59	546	01 16 56	–73 06 28	587	01 13 51	–73 04 19
506	01 15 50	–73 09 02	547	01 19 42	–73 05 19	588	01 12 07	–73 04 39
507	01 14 09	–73 09 33	548	01 17 19	–73 06 05	589	01 17 24	–73 02 57
508	01 16 38	–73 08 43	549	01 19 20	–73 05 17	590	01 13 29	–73 04 06
509	01 15 56	–73 08 55	550	01 14 15	–73 06 59	591	01 16 04	–73 02 39
510	01 16 48	–73 08 37	551	01 17 48	–73 05 45	592	01 18 56	–73 01 30
511	01 14 16	–73 09 23	552	01 15 50	–73 06 21	593	01 14 29	–73 03 02
512	01 16 22	–73 08 43	553	01 14 43	–73 06 39	594	01 15 58	–73 02 24
513	01 18 01	–73 08 05	554	01 19 56	–73 04 44	595	01 19 39	–73 00 59
514	01 17 16	–73 08 13	555	01 18 13	–73 05 20	596	01 17 28	–73 01 41
515	01 15 21	–73 08 51	556	01 12 23	–73 07 11	597	01 14 34	–73 02 32
516	01 18 11	–73 07 48	557	01 16 12	–73 05 47	598	01 19 42	–73 00 24
517	01 13 37	–73 09 10	558	01 17 56	–73 05 10	599	01 12 37	–73 02 40
518	01 20 07	–73 06 52	559	01 13 38	–73 06 34	600	01 16 08	–73 01 11
519	01 14 35	–73 08 49	560	01 19 34	–73 04 27	601	01 14 38	–73 01 34
520	01 13 60	–73 08 58	561	01 18 20	–73 04 47	602	01 12 05	–73 02 14
521	01 16 26	–73 08 12	562	01 15 60	–73 05 19	603	01 14 20	–73 01 32
522	01 16 33	–73 08 05	563	01 18 04	–73 04 35	604	01 12 21	–73 01 39
523	01 19 17	–73 06 48	564	01 16 42	–73 05 01	605	01 16 15	–73 00 22
524	01 17 53	–73 07 17	565	01 17 12	–73 04 44	606	01 19 60	–73 58 55
525	01 17 01	–73 07 35	566	01 19 06	–73 03 49	607	01 17 52	–73 59 44
526	01 17 46	–73 07 13	567	01 12 48	–73 05 48	608	01 13 20	–73 01 08
527	01 17 24	–73 07 19	568	01 18 01	–73 04 02	609	01 13 29	–73 01 06
528	01 15 59	–73 07 47	569	01 16 01	–73 04 41	610	01 15 41	–73 00 26
529	01 14 51	–73 08 08	570	01 16 19	–73 04 28			
530	01 13 13	–73 08 26	571	01 16 13	–73 04 28			
531	01 16 14	–73 07 29	572	01 15 15	–73 04 47			
532	01 12 13	–73 08 34	573	01 15 38	–73 04 34			
533	01 15 25	–73 07 37	574	01 18 45	–73 03 25			